Halide-Free Synthesis and Tribological Performance of Oil-Miscible Ammonium and Phosphonium-Based Ionic Liquids

A. Westerholt,[†] M. Weschta,[‡] A. Bösmann,[†] S. Tremmel,[‡] Y. Korth,[§] M. Wolf,[§] E. Schlücker,[∥]
N. Wehrum,[⊥] A. Lennert,[⊥] M. Uerdingen,[⊥] W. Holweger,[§] S. Wartzack,[‡] and P. Wasserscheid*,[†]

[†]Institute of Chemical Reaction Engineering, Friedrich-Alexander-University Erlangen-Nuremberg, Egerlandstraße 3, 91058 Erlangen, Germany

[‡]Institute of Engineering Design KTmfk, Friedrich-Alexander-University Erlangen-Nuremberg, Martensstraße 9, 91058 Erlangen, Germany

[§]Schaeffler Technologies GmbH & Co. KG, Industriestraße 1-3, 91074 Herzogenaurach, Germany

[∥]Institute of Process Machinery and Process Equipment, Friedrich-Alexander-University Erlangen-Nuremberg, Cauerstraße 4, 91058 Erlangen, Germany

[⊥]Merck KGaA, Frankfurter Straße 250, 64293 Darmstadt, Germany

S *Supporting Information*

ABSTRACT: Due to their low vapor pressures, nonflammability, high thermal stabilities, and excellent tribological properties ionic liquids (ILs) are highly attractive lubricant base oils and additives. However, for practical applications of ILs in lubrication, two requirements are often limiting, the required miscibility with standard mineral oils ($\geq$5 wt %) and the complete absence of corrosive halide ions in the ionic liquid. Moreover, the need for full compatibility with standard oil additives reduces the number of potential IL-based lubricant additives even further. In this contribution, an economic halide-free synthesis route to oil-miscible ionic liquids is presented, and very promising tribological properties of such ILs as base oil or additive are demonstrated. Therefore, sliding tests on bearing steel and XPS analysis of the formed surface films are shown. Corrosion test results of different bearing metals in contact with our halide-free ILs and (salt) water prove their applicability as real life lubricants. In the sustainable chemistry and engineering context, we present a halide-free design approach for ionic performance chemicals that may contribute to significant energy savings due to their enhanced lubrication properties.

KEYWORDS: *Ionic liquid, Halide-free, Lubrication, Oil-miscible, XPS, Noncorrosive*
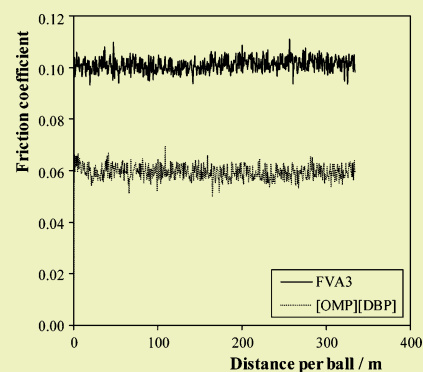
INTRODUCTION

Ionic liquids (ILs), salts with melting points below 100 °C, are characterized by a unique property profile including very low vapor pressure, electric conductivity, tunable coordination properties, and very attractive solvation power.[1] Most IL properties are a strong function of the individual ions that form the respective salt, for example, IL hydrophobicity, viscosity, toxicity, or coordination strength is strongly dependent on the IL's cation/anion combination.[2,3] By further chemical functionalization of the ions, the range of properties can be further expanded.

The first publication dealing with room temperature ionic liquids (RTILs) as lubricants was published in 2001 by Ye et al.[4] Following this seminal work, many groups have explored by "trial and error" testing[5] the potential of typical imidazolium-based ionic liquids, for example, $[NTf_2]^-$, $[BF_4]^-$, and $[PF_6]^{-6-10}$ salts, to act as lubricants or lubricant additives.[11] Due to some drawbacks identified with these structures, like high corrosion potential and manufacturing costs, more hydrolysis-stable, nonhalide forming salts like fluorinated alkyl

sulfates,[12] tetraalkyl borates,[13] and dialkyl phosphates were investigated later.[14-17] Due to the restricted number of halide-free ionic liquids displaying a high viscosity index (VI, namely, a low dependency of viscosity on temperature), lubrication research considered quickly the use of ionic liquids as additives to standard base oils.[18] In this context, miscibility of such additive ionic liquids in standard base oils becomes a very important requirement. Due to their salt structure, many traditional ILs show hardly any miscibility with commonly used nonpolar base oils, such as polyalphaolefins (PAO) or mineral oil cuts.[19]

In the above named studies on IL-based lubrication, a number of structural elements have been identified that qualify ionic liquids for good tribological performance.[5-20] These include (a) phosphorus- or boron-containing ions, (b) halide-free structure and halide-free synthesis of the ILs, (c) readily

available IL precursors, (d) additive compatibility, and (e) miscibility with common base oils. The relevance of phosphorus- or boron-containing ions like phosphonium cations[21] or borate,[13] phosphate,[16] phosphonate, and phosphinate[17] anions is due to the ability of these ions to form protective surface layers that reduce friction, wear, and corrosion.[13,16,17] The absence of any halide ion in the ionic liquid is mandatory, and low chloride content limits are given by the lubrication industry (0.5–50 ppm).[22] Also, traces of halide from the synthesis have to be excluded as it has been found that even very small amounts of halide drastically increase the corrosion potential of ionic liquids in combination with humidity.[23] Thus, synthetic routes to ILs that should serve as lubricants or lubricant additives should avoid any halides or halide impurities.

In contrast, suitable routes should use inexpensive and readily available halide-free IL precursors in high-yield transformation steps. The required miscibility of IL lubricant additives in common base oils is a key scientific challenge. It has been found by many research groups that long aliphatic substituents on the IL cation or the IL anion (or at both ions) lead to suitable solubility in base oils but also to high IL viscosity.[13,17,24−27] Consequently, the concept to add a small portion of IL additive to suitable base oils has become the major approach to improve lubrication performance by ionic liquids. For example, trihexyltetradecylphosphonium ($[P_{66614}]^+$)-based phosphate and phosphinate ILs were proposed as oil additives by Cytec Industries, Inc. The latter salt shows good oil-miscibility (up to 5 wt %), and its mixtures with base oils resulted in excellent tribological performance.[17,24]

However, this work applied a synthetic route for the synthesis of the $[P_{66614}]^+$ salts involving transformation of the $[P_{66614}]^+$ chloride or bromide salt with the respective phosphoric acid or phosphinic acid. In this reaction, sequence halide-contaminated products were obtained in the first place. Of course, these halide impurities can be reduced by washing the hydrophobic ILs with water. However, such cleaning steps are time consuming, generate excessive amounts of waste, and are limited in their ability to effectively remove all halide ions. Given the fact that it is very difficult to indicate—based on today's knowledge—a safe upper limit of acceptable halide impurities, it appears attractive to completely avoid the presence of halides in the synthetic sequence.

In this contribution, we describe a new, simple, and halide-free route to synthesize long alkyl chain-substituted ammonium and phosphonium ILs. Some of the synthesized structures here have been prepared previously using different halide-containing synthetic strategies.[15,28] Our new approach includes two steps. In the first step, a long chain alkyl-substituted amine or phosphine is alkylated using trimethylphosphate as the alkylating agent (Figure 1).

As a second step to further increase oil-miscibility (while decreasing water solubility at the same time), the dimethyl phosphate anion is exchanged by addition of a Brønsted acid derived from a more hydrophobic acid as shown in Figure 2.

The protonated dimethyl phosphate anion and remaining phosphoric acid can be washed out easily with a mixture of distilled water and triethylamine. Halide-free anion exchange reactions are well known in the literature,[1,29−31] for example, by reaction of dimethyl carbonate or hydroxide with acids. The new aspect of our synthesis is that we realize a similarly facile halide-free anion exchange without applying the weak alkylation agent dimethyl carbonate in the first step[32,33] or without the
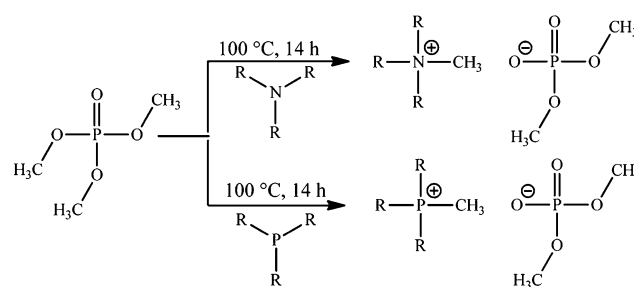

Figure 1. Alkylation of trialkylamine or trialkylphosphine with trimethylphosphate as the first step of our two-step reaction sequence to synthesize oil-miscible ionic liquids in a halide-free manner.
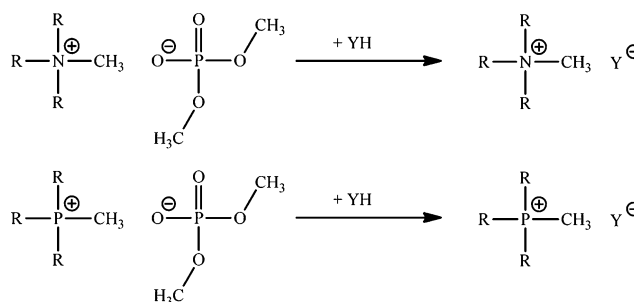

Figure 2. Anion exchange from ammonium or phosphonium dimethyl phosphate to longer alkyl chain anions by the use of a hydrophobic Brønsted acid.

need to introduce the hydroxide ion via an ion exchange column or a membrane process.[34]

In the first step of our two-step synthesis sequence, three different precursor ILs have been prepared, namely, trioctylmethylammonium dimethyl phosphate [OMA][DMP], tridodecylmethylammonium dimethyl phosphate [DMA][DMP], and trioctylmethylphosphonium dimethyl phosphate [OMP]-[DMP]. All three ionic liquids have been obtained in very high yields (see the Supporting Information for analytical details), and all of them emulsify with water.

In the described second step of the sequence, these salts have been converted to dibutyl phosphates and bis(2,4,4-trimethylpentyl) phosphinates as shown in Table 1.

The results of the tribological performance tests using these ionic liquids are compared to the commercial oil-miscible IL trihexyltetradecylphosphonium bis(2,4,4-trimethylpentyl) phosphinate $[P_{66614}][BMPP]$ from Cytec Industries, Inc. that has been obtained in a synthesis using the respective chloride salt as intermediate. In order to show synthesis-dependent effects, we performed thermal stability and wettability studies and also corrosion tests.

■ EXPERIMENTAL SECTION

Applied Chemicals and IL Synthesis. The applied chemicals together with their purities and suppliers are listed in Table 2.

General Synthesis Procedures (All Analytical Details Are Given in the Supporting Information). *Synthesis of [DMP]-ILs (Precursor ILs).* A biphasic mixture of 1.0 equiv amine (or phosphine) and 1.2 equiv trimethyl phosphate was intensely stirred for 14 h at 100 °C under reflux. The excess trimethyl phosphate was removed by vacuum distillation to obtain the ionic liquid as a yellow (or colorless) liquid.

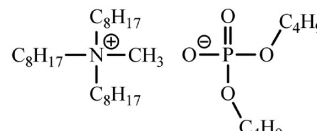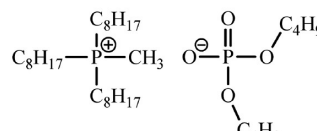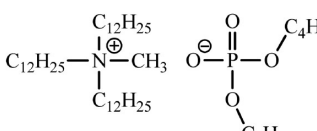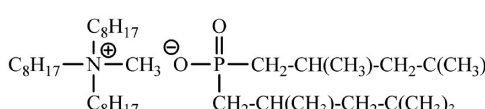**Table 1. Structures, Names, and Abbreviations of Examined Ionic Liquids**

Trioctylmethylammonium dibutyl phosphate [OMA][DBP]

C_8H_{17}—$N^{\oplus}(C_8H_{17})(CH_3)$—$C_8H_{17}$ $O^{\ominus}$—$P(=O)(OC_4H_9)$—O—C_4H_9
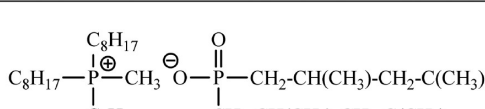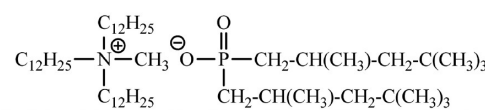
Trioctylmethylphosphonium dibutyl phosphate [OMP][DBP]

C_8H_{17}—$P^{\oplus}(C_8H_{17})(CH_3)$—$C_8H_{17}$ $O^{\ominus}$—$P(=O)(OC_4H_9)$—O—C_4H_9

Tridodecylmethylammonium dibutyl phosphate [DMA][DBP]

$C_{12}H_{25}$—$N^{\oplus}(C_{12}H_{25})(CH_3)$—$C_{12}H_{25}$ $O^{\ominus}$—$P(=O)(OC_4H_9)$—O—C_4H_9

Trioctylmethylammonium bis(2,4,4-trimethylpentyl) phosphinate [OMA][BMPP]

C_8H_{17}—$N^{\oplus}(C_8H_{17})(CH_3)$—$C_8H_{17}$ $O^{\ominus}$—$P(=O)$—CH_2-$CH(CH_3)$-CH_2-$C(CH_3)_3$ / CH_2-$CH(CH_3)$-CH_2-$C(CH_3)_3$

Trioctylmethylphosphonium bis(2,4,4-trimethylpentyl) phosphinate [OMA][BMPP]

C_8H_{17}—$P^{\oplus}(C_8H_{17})(CH_3)$—$C_8H_{17}$ $O^{\ominus}$—$P(=O)$—CH_2-$CH(CH_3)$-CH_2-$C(CH_3)_3$ / CH_2-$CH(CH_3)$-CH_2-$C(CH_3)_3$

Tridodecylmethylammonium bis(2,4,4-trimethylpentyl) phosphinate [DMA][BMPP]

$C_{12}H_{25}$—$N^{\oplus}(C_{12}H_{25})(CH_3)$—$C_{12}H_{25}$ $O^{\ominus}$—$P(=O)$—CH_2-$CH(CH_3)$-CH_2-$C(CH_3)_3$ / CH_2-$CH(CH_3)$-CH_2-$C(CH_3)_3$

Table 2. Chemicals

substance	supplier	purity
trioctylamine	Merck KGaA	for synthesis
tridodecylamine	Merck KGaA	for synthesis
trioctylphosphine	ABCR GmbH & Co. KG Merck KGaA	97%
trimethyl phosphate	Merck KGaA	for synthesis
dibutyl phosphate	Alfa Aesar	96%
bis(2,4,4-trimethylpentyl) phosphinic acid	Cytec Industries, Inc.	85%
trihexyltetradecyl phosphonium bis(2,4,4-trimethylpentyl) phosphinate	Cytec Industries, Inc.	for synthesis
triethylamine	Merck KGaA	for synthesis

Yields: [OMA][DMP] > 99.9%,

[OMP][DMP] > 99.9%,

[DMA][DMP] > 99.9%

Synthesis of [DBP] and [BMPP] ILs. A total of 1.4 equiv triethylamine was added to a cooled mixture of 1.2 equiv of the acid compound and 1.0 equiv of the precursor IL. The mixture was stirred 3 h at room temperature before distilled water was added. After intensely stirring the biphasic mixture for 3 h, the organic phase was separated, washed once with a triethylamine−distilled water solution,

and washed twice with distilled water. Finally, the IL was dried at 60 °C under vacuum conditions (<0.1 mbar) for 12 h.

Yields: [OMA][DBP] 99%, [OMP][DBP] 99%,

[DMA][DBP] 99%, [OMA][BMPP] 99%,

[OMP][BMPP] 99%, [DMA][BMPP] 99%

Physical Properties. *Viscosity and Density.* All measurements were carried out with dried samples of defined water contents (Table 3). The latter was previously determined by a Metrohm 756 Karl Fischer coulometer using a Hydranal Coulomat AG reagent.

Table 3. Compositions of Lubricant Samples Tested within This Study

Sample	Ingredients	water content	
1	[OMA][DBP]	1100 ppm	
2	[OMP][DBP]	1200 ppm	
3	[DMA][DBP]	600 ppm	
4	5 wt% [OMA][DBP] in FVA3		
5	5 wt% [OMP][DBP] in FVA3		Blends
6	5 wt% [DMA][DBP] in FVA3		
7	5 wt% [OMA][BMPP] in FVA3		
8	5 wt% [OMP][BMPP] in FVA3		
9	5 wt% [DMA][BMPP] in FVA3		
10	FVA3		
11	FVA4		
12	[P$_{66614}$][BMPP]	700 ppm	
13	5 wt% [P$_{66614}$][BMPP] in FVA3		

The viscosities were determined using a MCR 100 rheometer from Anton Paar. Temperature in the rheometer was controlled by a Peltier element. Densities were measured in the oscillating U-tube density meter DMA 5000 M from Anton Paar.

Thermal Stability. Thermogravimetric measurements were carried out using a SETSYS evolution TGA from Setaram. The samples were heated from room temperature to 500 °C with a heating ramp of 10 K/min in a helium atmosphere. Decomposition temperatures were determined as onset temperatures of the decomposition curves.

Wettability. Contact angles were measured on polished bearing steel (100Cr6, AISI 52100) and stainless steel (V4A, AISI 316Ti) using a DSA100 from Krüss at 30 and 70 °C.

Tribological Performance. The applied balls and polished disks were made of bearing steel (100Cr6, AISI 52100). Due to their long alkyl chain substituents, the ILs [OMA][BMPP], [OMP][BMPP], and [DMA][BMPP] show grease-like consistency. Consequently, these substances were investigated as 5 wt % additives in a FVA3 reference oil. FVA reference mineral oils [reference oil of the Forschungsvereinigung Antriebstechnik e.V. (http://fva-net.de)] include no additives and can be commercially obtained in four different viscosity classes (FVA1−4). The other three [DBP] ILs were tested as both pure base oils and additives in FVA3. The compositions of all tested lubricant samples are listed in Table 3.

Sliding Tests. Tribological performance was examined using a three-ball-on-disk test with a Wazau TRM 1000 tribometer.

As shown in Figure 3, three fixed balls are in contact during this test with the disk, which is completely covered by the lubricant sample. A cardan joint guarantees a symmetric tribo contact controlled by a distance-amplifying instrument. For all experiments, the sliding conditions listed in Table 4 have been kept constant.
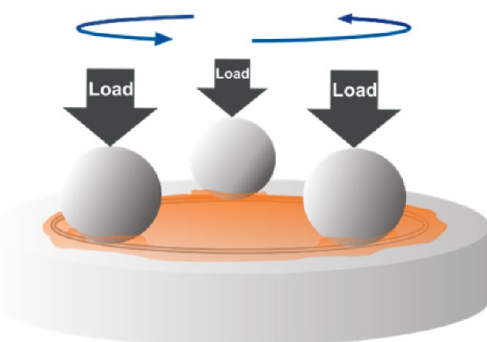
Figure 3. Scheme of the sliding test.

Table 4. Conditions of the Sliding Tests

sliding speed (m/s)	0.2
ball diameter (mm)	8
temperature (°C)	22
load (N)	195 per ball
time (s)	1668
distance (m)	1000 (333.3 per ball)

The sliding tests were repeated three times for all samples. For each disk, the wear tracks were examined using a 3D-laser scanning microscope from Keyence (VK-X200 series). Four pictures of each circular wear track were taken in 90° distance Cross-sectional profiles were generated, and wear losses were calculated. Due to the large ball diameter, mostly no wear tracks were visible on the ball surfaces.

Corrosion. The corrosivities of the ILs [OMA][DBP] and [OMP][DBP] were tested on four different metals, namely, steel (100Cr6, AISI 52100), stainless steel (V4A, AISI 316Ti), brass, and construction steel (St12−03, DC01). Prior to the corrosion experiments, the metal surfaces of all samples were cleaned by grinding with abrasive paper (grit: 100 and 320) followed by degreasing with cyclohexane in an ultrasonic bath for 30 min and washing with distilled water and acetone. After drying, all samples were weighed and afterward contacted for 7 days at 70 °C with pure IL (Figure 4), with IL + distilled water, or with IL + salt water (Figure 5).
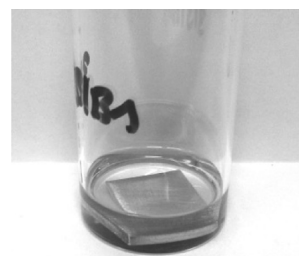
Figure 4. Corrosion test with pure IL.

Figure 5. Corrosion test with IL and distilled or salt water.

After exposure of the metal samples to the corrosion experiments, the samples were washed with cyclohexane, acetone, and dichloromethane. After drying, the sample weight loss was determined. For optical corrosion analysis, pictures of all samples were taken using an optical microscope.

RESULTS AND DISCUSSION

Viscosity. Due to the fact that all tribological setup parameters are kept constant during the experiments, only the viscosity and the lubricant composition are held responsible for the tribological performance changes.

According to Stribeck[35], variation of the viscosity could lead to a change of the tribological regime by affecting the internal friction and stability of the lubrication film. To exclude this viscosity influence, densities and viscosities of all samples were determined prior to lubrication tests (Table 5). Comparing the

Table 5. Kinematic Viscosities (mm²/s) of Pure ILs, Reference Oils, and 5 wt % IL−FVA3 Blends

Sample	T / °C						
	0	10	20	40	60	80	
1	23820	9245	4047	946	291	110	ILs
2	4095	1715	800	223	82	38	
3	45052	16027	6521	1383	400	147	
4	1400	646	323	101	42	21	
5	1340	606	299	94	39	20	
6	1316	614	309	98	40	20	blends
7	1445	656	322	100	41	20	
8	1392	644	319	100	41	21	
9	1392	644	319	100	41	21	
10	1441	656	324	101	41	21	
11	14557	5083	2128	512	169	70	Reference
12	6672	3390	1759	595	246	117	
13	1415	643	326	103	42	25	

tribological performance of lubricants with similar viscosities allowed for reducing the influence parameter of the lubricant composition.

Remarkably, the viscosities of all IL−FVA3 blends (Table 5, entries 4−9) are in the same range as the measured viscosity of the pure reference oil FVA3 (Table 5, entry 10). This allows a comparison of the sliding test results of the IL blends with those of pure FVA3. Figure 6 visualizes the temperature dependency of the kinematic viscosities for the pure ILs in comparison to the two different FVA reference oils.
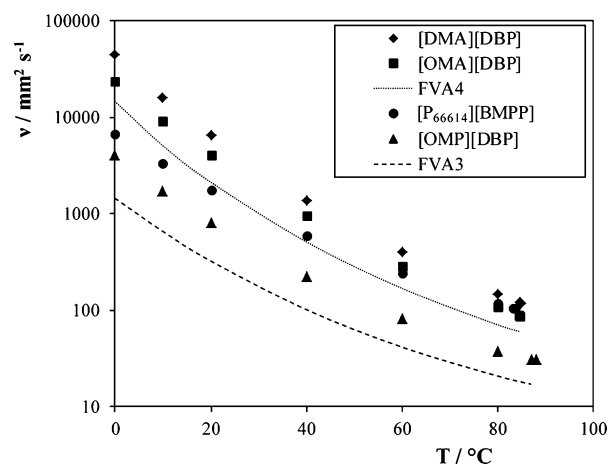
Figure 6. Kinematic viscosities of the studied pure ILs and of the two FVA reference oils plotted on a logarithmic scale.

All pure ILs under investigation have a significant higher viscosity than the reference oil FVA3. Therefore, their tribological properties will be compared to the reference oil FVA4 of similar viscosity. The expected viscosity reducing effect of phosphonium cations[36] is indeed observable by comparing the viscosity curves of the structure-analogous ILs [OMA][DBP] and [OMP][DBP]. Also, the expected increase in viscosity by increasing the lengths of aliphatic substituents can be observed for all pure phosphonium and ammonium ILs (e.g., compare the viscosities of [OMA][DBP] and [DMA]-[DBP]).

Wettability. Besides viscosity, wettability also is an important parameter for the formation of a stable lubrication film on a metal surface.[37] The relevant parameter to characterize the ability of a liquid to cover a surface is its contact angle (Θ). Contact angles below 45° indicate a good wetting behavior of the respective liquid. In Figures 7 and 8, the
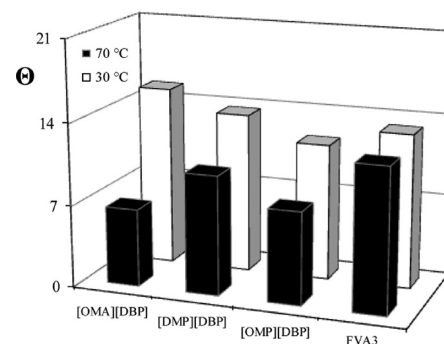
Figure 7. Averaged contact angles on bearing steel.

contact angles of FVA3 and the pure [DBP] ILs on bearing steel and on stainless steel at 30 and 70 °C are presented. To avoid surface influences on the metal contact (grooving, dust), polished disks were used after thorough cleaning with compressed air.
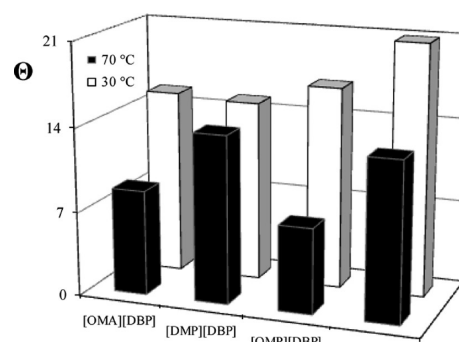
Figure 8. Averaged contact angles on stainless steel.

All measured ILs show an excellent wetting behavior with contact angles far below 45° and comparable to FVA3. In addition, the tested ammonium and phosphonium [DBP] ILs show a slightly better wettability for stainless steel than the ammonium bis(trifluorosulfonylimide) ILs published by Qu et al.[26]

Thermal Stability. Thermal stability tests were carried out to compare the stability of the pure IL with the standard reference oil FVA3. Note that the applied heating ramp of 10 K/min overestimates the absolute thermal stability of all tested compounds.[38] However, the method still allows a reliable and efficient comparison of the thermal stability of all samples. The results obtained under identical testing conditions are listed in Table 6.

Table 6. Results of TGA Thermal Stability Tests for Pure ILs and Reference Base Oil FVA3 Using a Heating Ramp of 10 K/min

IL	$T_{decomp.}$/°C	IL	$T_{decomp.}$/°C
[OMA][DBP	239	[OMA][BMPP]	252
[OMP][DBP]	320	[OMP][BMPP]	352
[DMA][DBP]	261	[DMA][BMPP]	273
FVA3	309	[P$_{66614}$][BMPP]	343 (366[17])

As expected, the thermal stability of the phosphonium-based ILs is significantly higher than that of their ammonium counterparts. Bradaric et al.[39] have suggested that this difference originates from different decomposition mechanisms. While ammonium ions decompose via Hoffmann- or β-eliminations, phosphonium ion decomposition happens by formation of tertiary phosphonium oxides or stable phosphoranes (Wittig reagent).

Friction Coefficients. In Figures 9−11, the friction coefficients recorded during the 1000 m sliding tests for the
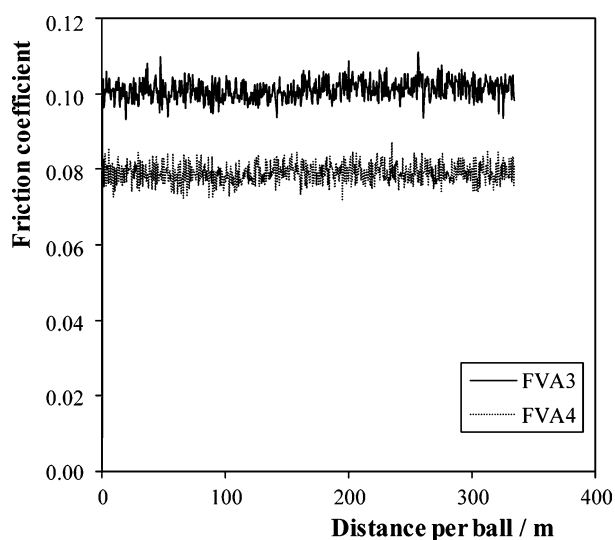
Figure 9. Friction coefficients of the standard base oils FVA3 and FVA4.

reference oils and the IL blends are shown. First, the friction coefficients of the pure reference base oils, FVA3 and FVA4, are compared. The friction coefficient of FVA4 is slightly lower than that of FVA3, and what can be concluded is a better lubricant film formation due to the higher viscosity and
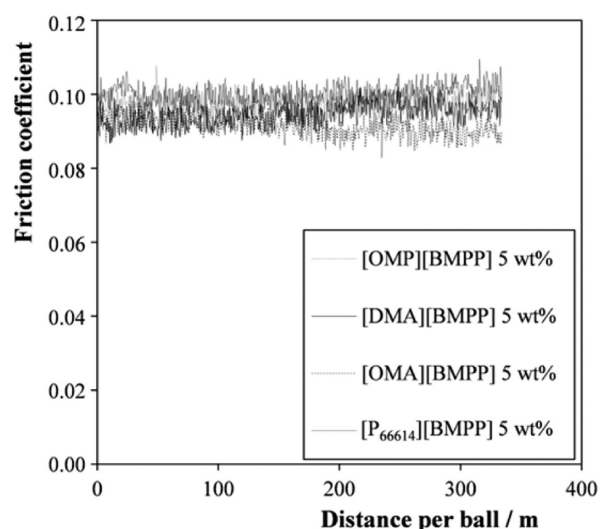
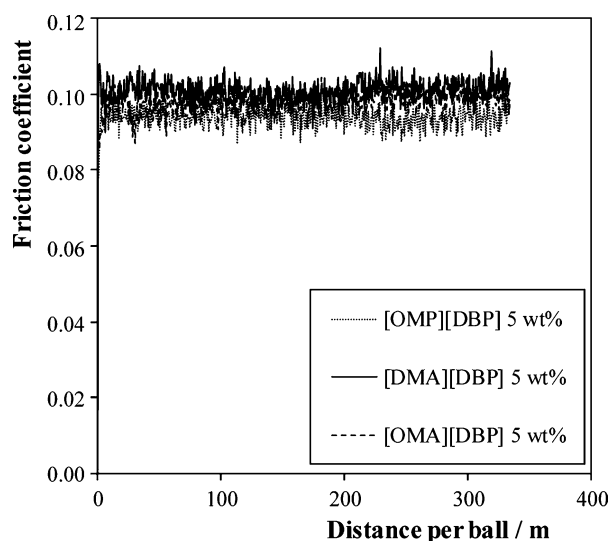**Figure 10.** Friction coefficients of different [BMPP] IL−FVA3 blends.

Figure 11. Friction coefficients of different [DBP] IL−FVA3 blends.

therefore less mixed lubrication. An increase in fluid friction with higher viscosity comparably seems to be of lower impact.

As all IL blends are composed of a 95 wt % share of FVA3 (Table 5), their viscosities are very similar to FVA3. Therefore, we conclude that the small friction improvements observed for the blends with [OMA][BMPP] (Figure 10) and [OMP]-[DBP] (Figure 11) are directly caused by a positive tribological influence of the respective IL additive.

The friction coefficients of the pure ILs under investigation in this study are presented in Figures 12−15 in comparison with the FVA reference oil of comparable viscosity to avoid viscosity effects on the relative lubrication performance.

All pure ILs have lower average friction coefficients compared to their blends or the pure FVA oils. The obtained friction coefficients of the pure ILs decrease in the following order: [P$_{66614}$][BMPP] > [OMA][DBP] > [DMA][DBP] > [OMP][DBP]. Thus, the different [DBP] ILs show better friction reducing performance compared to [P$_{66614}$][BMPP]. The friction slightly decreases with increasing alkyl chain lengths of the cation substituents corresponding to the viscosity increase from [OMA][DBP] to [DMA][DBP]. A remarkable result shows the IL [OMP][DBP]. This IL shows the best
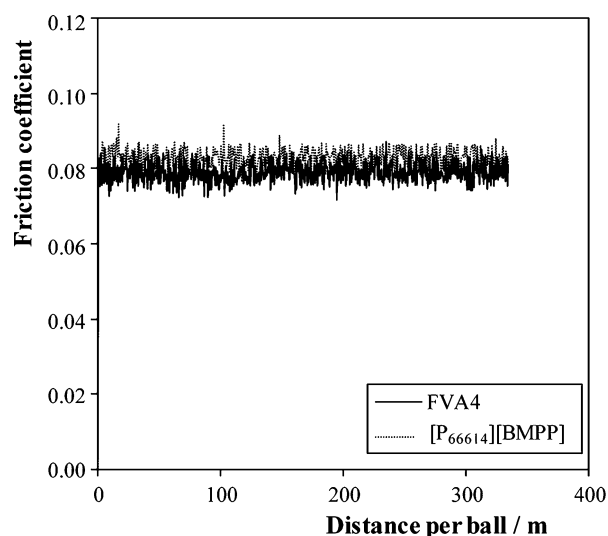
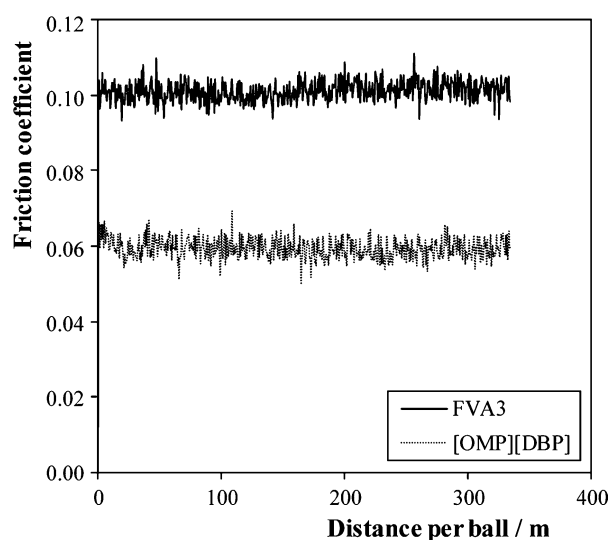**Figure 12.** Friction coefficients of FVA4 and [P$_{66614}$][BMPP].

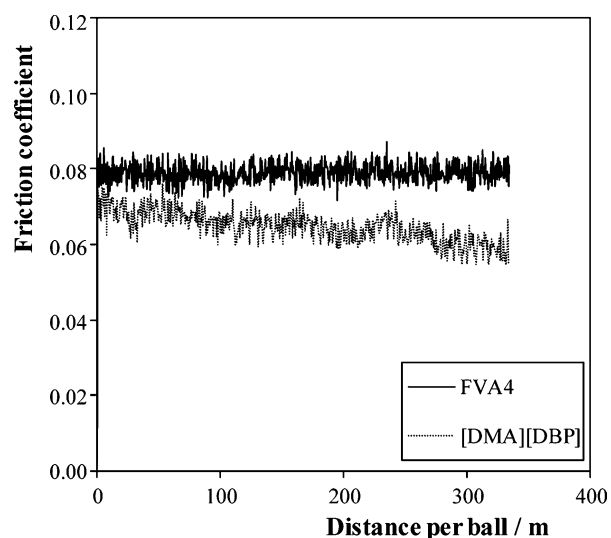**Figure 13.** Friction coefficients of FVA3 and [OMP][DBP].

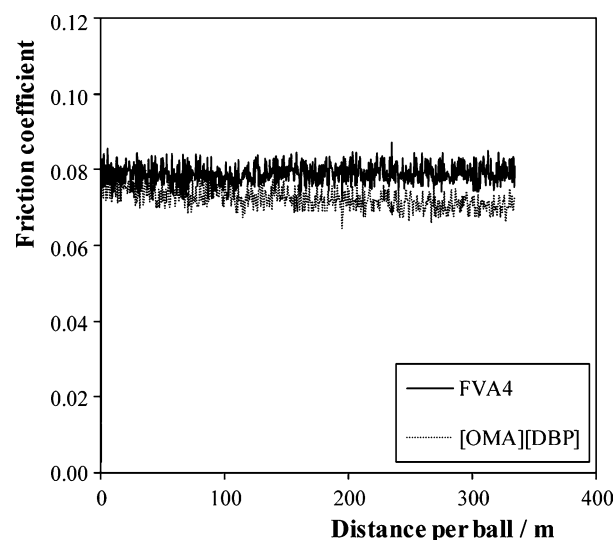**Figure 14.** Friction coefficients of FVA4 and [DMA][DBP].

Figure 15. Friction coefficients of FVA4 and [OMA][DBP].

constant frictional behavior with an averaged friction coefficient of 0.06. Remarkably, in comparison to the much more viscous FVA3, the friction coefficient is reduced by 40%. Moreover, [OMP][DBP] shows a better frictional behavior than [OMA]-[DBP] despite its lower viscosity.

As shown in Figure 14 and slightly in Figure 15, the friction coefficients of the ammonium-based ILs are still going down after 1000 m. To study this behavior in more detail, an extended sliding test over a distance of 5000 m has been carried out with [OMA][DBP]. Figure 16 shows that the friction coefficient reduces even more with increased sliding distance.
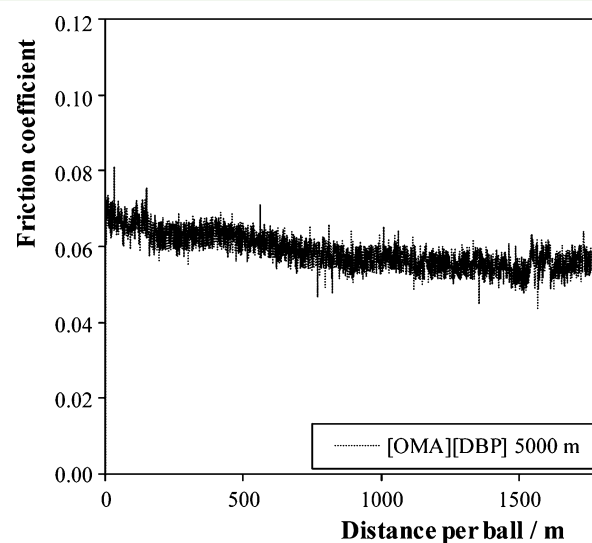

Figure 16. Friction coefficients of [OMA][DBP] reported for 5000 m distances.

Qu et al.[26] postulated that ammonium ILs show low friction coefficients due to their ability to react very fast with the freshly produced surfaces resulting from material removal and deformation processes at the sliding contact. These authors support their hypothesis with an acceleration of the wear process that they concluded from high wear volumes found in their measurements. To find out whether such deformation processes by abrasion or adhesion on the metal surface play any

role for our measurements, we determined wear and bulging coefficients for all lubricants under investigation in this study (Table 7).

Table 7. Averaged Friction and Wear Coefficients (Sample Number $n = 3$)

Test ID	Averaged friction coefficient	Averaged wear coeff. mm³ N⁻¹ m⁻¹ (· 10⁻⁹)	Averaged bulge coeff. mm³ N⁻¹ m⁻¹ (· 10⁻⁸)	
1	0.07	2.18	0.12	
1b*	0.06	0.85	0.25	ILs
2	0.06	6.60	0.66	
3	0.07	3.12	0.07	
4	0.10	8.23	0.30	
5	0.09	3.95	1.46	
6	0.10	3.70	0.12	Blends
7	0.09	4.43	0.29	
8	0.10	6.36	2.64	
9	0.10	5.34	4.95	
10	0.10	6.80	3.56	
11	0.08	2.76	1.14	Reference
12	0.08	7.28	1.69	
13	0.10	6.20	5.87	

*Sliding distance = 5000 m.

From these data we can exclude from the relatively small wear coefficients for [OMA][DBP] that extended consumption of fresh metal takes place for this IL. In contrast, the slight increase in the bulge coefficient (0.12×10^{-8} to 0.25×10^{-8} mm³ N^{1-} m^{-1}) could be correlated to a slow decomposition of [OMA][DBP] at the sliding contact forming a stabile protection layer on the metal surface that prohibits friction and wear.

XPS Analyses of Sliding Traces. To shed more light on the mechanisms of IL-induced tribological effects with the ionic liquids under investigation, we examined samples from the 1000 m sliding tests with pure [OMA][DBP], [DMA][DBP], and [OMP][DBP] by XPS (Figures 17−24) [All XPS experiments were carried out by W. Dreher and K. Gerlach at the Institute of the Natural and Medical Sciences Institute (NMI) at the University of Tübingen.]

Indeed, the XPS spectra show the formation of phosphor- and oxide-containing protection layers. All three sliding traces show an increase in the O 1s peak at 532 eV and the formation of a new phosphorus species at 133 eV. This results are in good
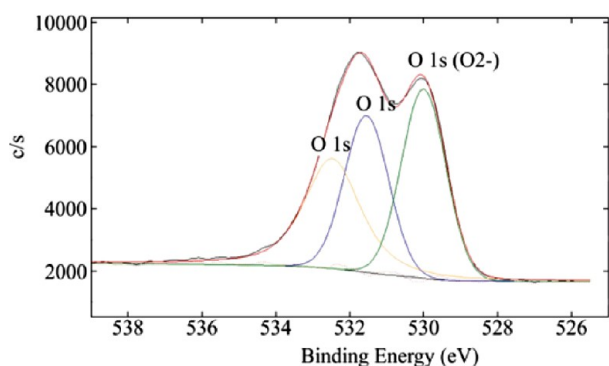

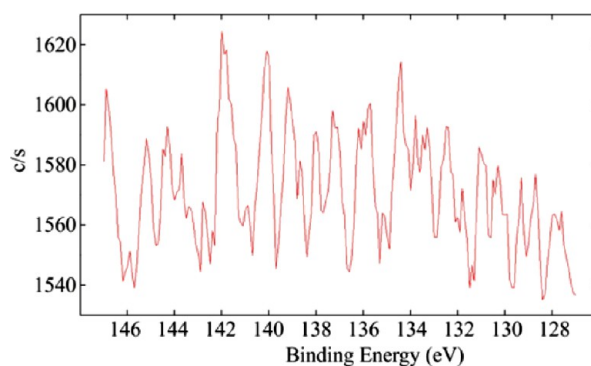**Figure 17.** O 1s XPS reference spectra of a blank disk before testing.

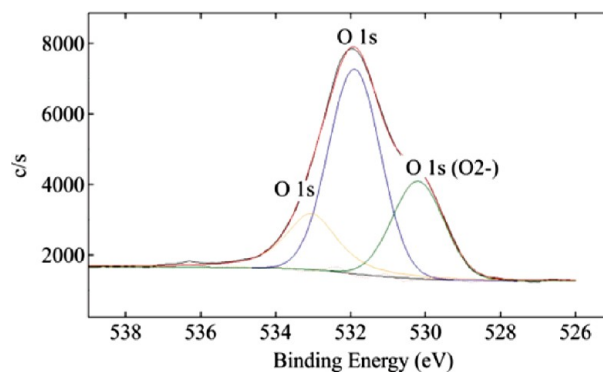**Figure 18.** P 2p XPS reference spectra of a blank disk before testing.

Figure 19. O s XPS spectra in the sliding trace of the [OMA][DBP] test.
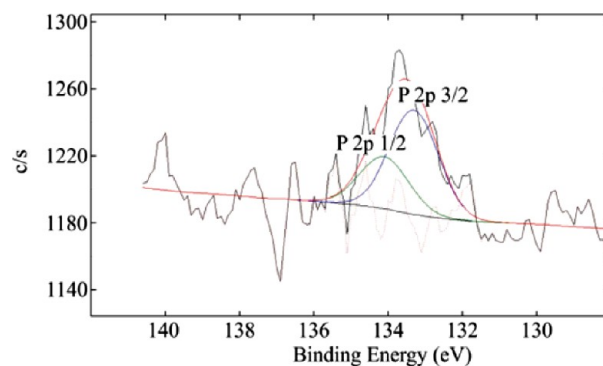

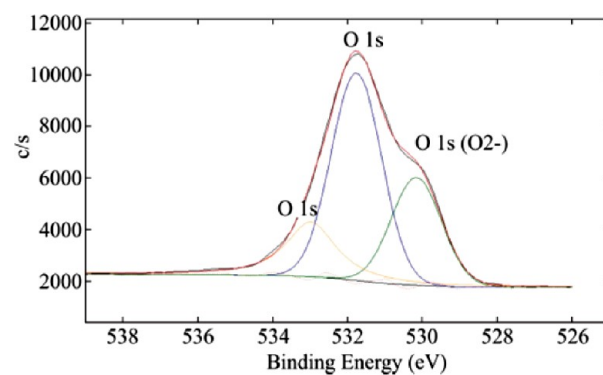**Figure 20.** P 2p XPS spectra in the sliding trace of the [OMA][DBP] test.

Figure 21. O1 s XPS spectra in the sliding trace of the [DMA][DBP] test.
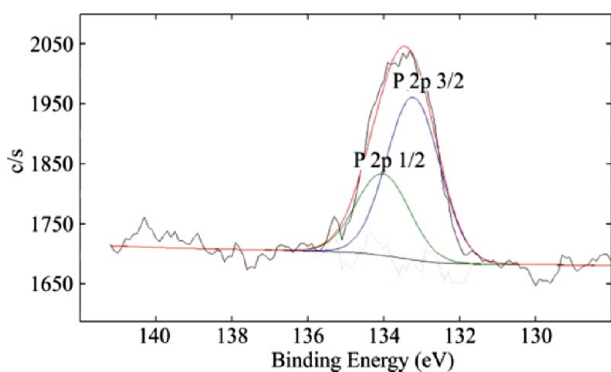
Figure 22. P 2p XPS spectra in the sliding trace of the [DMA][DBP] test.
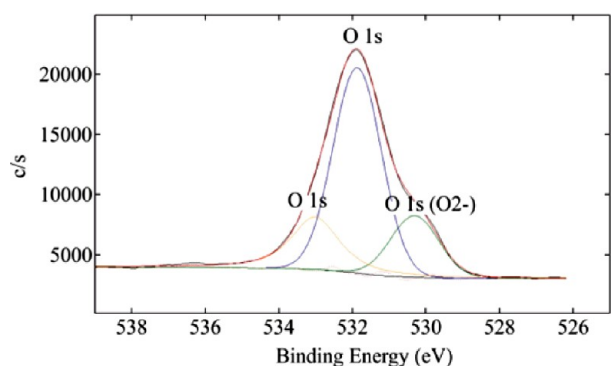

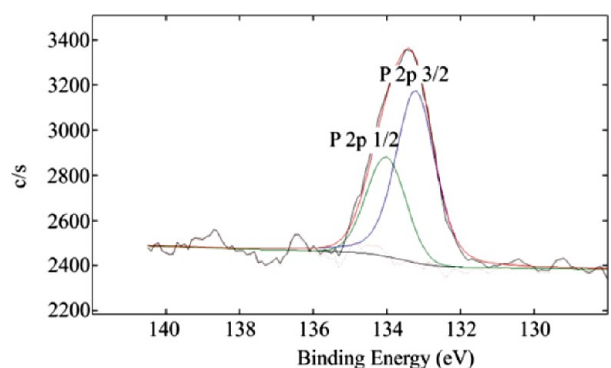**Figure 23.** O1 s XPS spectra in the sliding trace of the [OMP][DBP] test.

Figure 24. P 2p XPS spectra in the sliding trace of the [OMP][DBP] test.

Figure 25. (a) P 2p XPS mapping spectra of the blank disk before testing. (b) P 2p XPS mapping in the sliding trace of the [OMP][DBP] test.

agreement with reports by Zhang et al.,[16] who observed the formation of a protective layer on a steel surface with 1-octyl-2-ethylimidazolium diethyl phosphate. These authors correlated the observed O 1s (531.2 eV) and P 2p (133.7 eV) peaks in the XPS spectra to the formation of $Fe[PO_4]$.

Besides the composition of the protective layer, the XPS spectra indicate that the ability to form a protective layer after a 1000 m sliding distance differs among the different ILs. For example, the latter is higher for [OMP][DBP] than for [OMA][DBP]. Therefore, only the sliding traces of [OMP]-[DBP] show small signals in the P 2p XPS mapping analysis (Figure 25b). The observed small highlighted white spots represent phosphorus atoms located at the border of the protective layer.
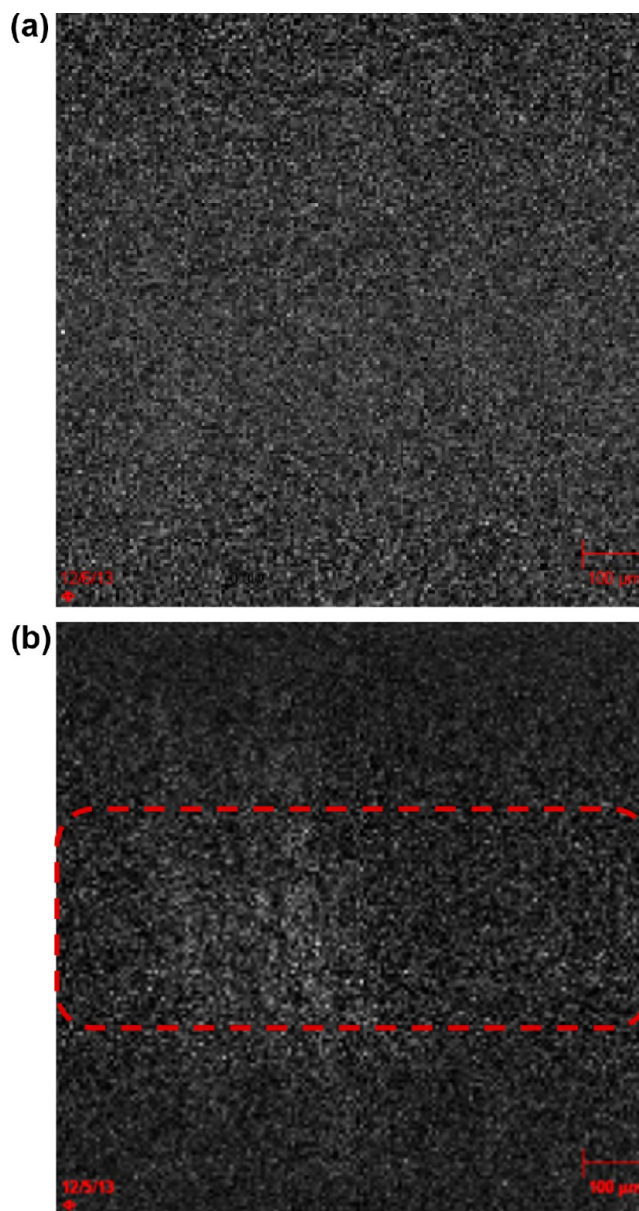
Corrosion Studies. In addition, corrosion tests have been carried out to determine the effect of [OMA][DBP] and [OMP][DBP] on the corrosion of construction steel (St-12), bearing steel (100Cr6), brass, and stainless steel (V4A). The test results for pure IL, distilled water + IL, and salt water + IL are presented in Table 8.

The results of the corrosion tests demonstrate the very low effect of both pure ILs [OMA][DBP] and [OMP][DBP] on corrosion with the tested metals. Uerdingen et al.[40] showed in mechanic stress tests that pure ILs are hardly corrosive to metals except for nonferrous metals like brass. Inline with our findings, these authors had earlier demonstrated that IL-induced corrosion increases dramatically by adding distilled water to the IL. In the case of [OMA][DBP] and [OMP]-[DBP], water addition leads to less severe corrosion effects than those observed by Uerdingen et al.[40] with the ILs

Table 8. Weight Loss* of Different Metal Samples in Our Corrosion Test over 7 d at 70 °C

		pure IL	IL + dist. water	IL + salt water	dist. water	salt water
[OMA][DBP]	St12	0.02	0.31	0.29	–	–
	100Cr6	0.00	0.16	0.31	–	–
	brass	0.00	0.17	0.10	–	–
	V4A	0.01	0.00	0.00	–	–
[OMP][DBP]	St12	0.00	0.11	0.09	–	–
	100Cr6	0.00	0.09	0.11	–	–
	brass	0.00	0.02	0.07	–	–
	V4A	0.00	0.00	0.00	–	–
ref. without IL	St12	–	–	–	0.02	0.15
	100Cr6	–	–	–	0.00	0.11
	brass	–	–	–	0.00	0.06
	V4A	–	–	–	0.00	0.00

*Weight loss of the metal sample = (weight difference in mg)/(surface area in cm^2)/(number of days).

ECOENG212, [EMIM][TOS], [BMIM]Cl, ECOENG418, ECOENG111P, AMMOENG100, and Tegotain3300.

Our hypothesis is that the hydrophobicity and water stability of [OMA][DBP] and [OMP][DBP] avoids formation of corrosive byproducts from the IL. Such corrosive byproducts, for example, phosphoric acid, were postulated in the work by Uerdingen et al.[40] Note that the ILs of this work form liquid–liquid biphasic systems with water or salt water. Thus, the metal sample is always in contact with a less dense liquid IL phase and a dense water-rich liquid phase.

All perfomed tests were executed without any mechanical or tribological stress. Tribo-corrosion tests are highly recommended for further investigations to explore the tribo-corrosion potential of both ILs, for example, compared to [P$_{66614}$][BMPP] obtained from halide-based synthesis routes.

As shown in Figure 26, salt water promotes corrosion on metals more than distilled water. This effect is observed for
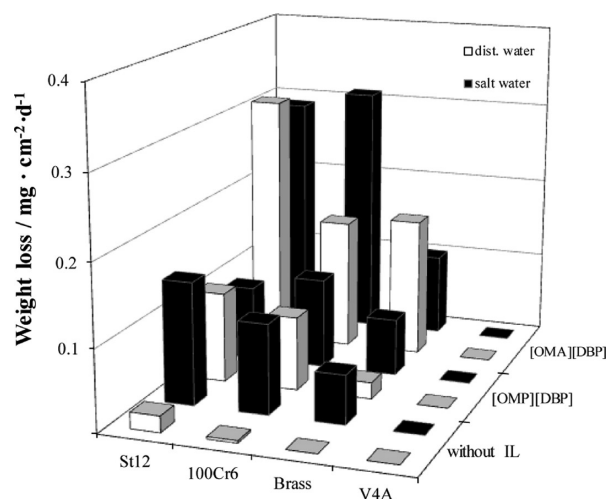

Figure 26. Weight loss of metals in the ILs [OMA][DBP] and [OMP][DBP] neat, with addition of water and with addition of salt water.

both ILs and for the test without IL. Remarkably, the relative difference in corrosivity between water-containing and salt water-containing tests is smaller with both ILs compared to the tests without IL. From this, we conclude that the presence of [OMA][DBP] and [OMP][DBP] protects the surface to some extent from chloride attack. Figure 27 summarizes the corrosion results by photographs and microscopic pictures of

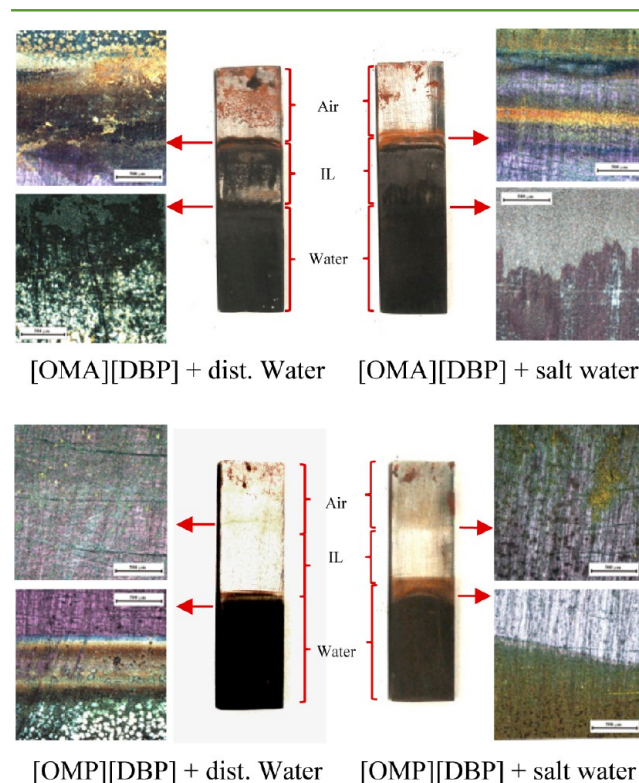the air–IL and IL–water boundaries for the IL + water corrosion tests on bearing steel.

Figure 27. IL + water corrosion tests on bearing steel with [OMA][DBP] and [OMP][DBP] ILs (microscopic pictures scale = 500 μm).

All corrosion tests occurred in closed beakers that were held at 70 °C for 7 days. Due to the humidity in the cabinet from the added water, the upper air-contacted part of the bearing sample started to rust. Note, however, that the IL-covered surfaces in the middle of the [OMP][DBP] samples are completely unscathed. The areas protected with [OMA][DBP] do not show visible corrosion, but the metal starts to tarnish. As expected, the areas contacted by pure distilled or salt water on the bottom of the sample were intensely corroded.

Brass is a zinc- and copper-containing alloy and tends to show selective leaching with the less noble metal zinc being more prone to dissolution. The more noble metal copper

precipitates on the corroded metal by coloring the surface from yellow to red.

As shown in Figure 28, by comparison of the IL—brass vs the water—brass contact area, [OMA][DBP] and [OMP][DBP] protect the brass surface and diminish selective leaching of zinc.
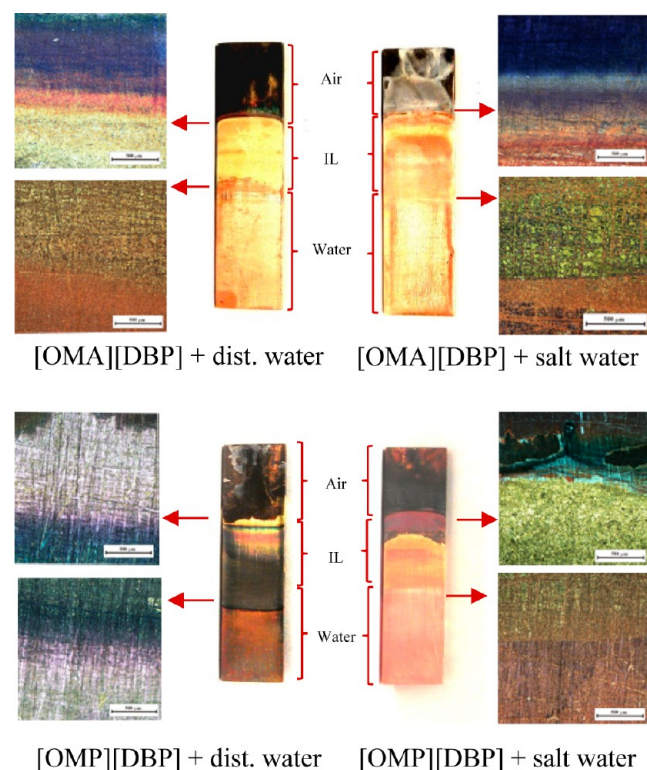

[OMA][DBP] + dist. water   [OMA][DBP] + salt water

[OMP][DBP] + dist. water   [OMP][DBP] + salt water

Figure 28. Water—IL corrosion tests on brass with [OMA][DBP] and [OMP][DBP] ILs (microscopic pictures scale = 500 μm).

The water covered parts of all brass samples show a strong red discoloration. The parts in contact with the IL [OMA]-[DBP] show, however, no corrosion. Beside tarnishing, the same beneficial behavior is found also for [OMP][DBP]. All samples form rust in air contact. In contrast to the study performed by Uerdingen et al.[40] with the ILs ECOENG212, [EMIM][TOS], [BMIM]Cl, ECOENG418, ECOENG111P, AMMO-ENG100, and Tegotain3300, we found no evidence of corrosion or selective leaching (Figure 29a and b) using the ILs [OMA][DBP] and [OMP][DBP].

CONCLUSIONS

A new synthesis route for halide-free, oil-miscible ILs has been presented in this work. The route comprises two steps and involves a phosphate ion exchange reaction as the key step. The route has several advantages over the reported state-of-the-art,[15] namely, that it (a) avoids very toxic alkylation agents (such as, for example, dimethyl sulfate), (b) avoids extensive heating at temperatures exceeding 120 °C, and (c) avoids any involvement of halides in the synthesis thus avoiding as well any cleaning procedures to remove halide traces.

The so-prepared phosphate and phosphinate ILs show remarkable tribological performances with low friction coefficients and wear volumes. Using XPS analyses, we could demonstrate that an iron phosphate protective layer is formed on the sliding traces. Our sliding tests also show that ammonium ILs need more time to create a protective layer
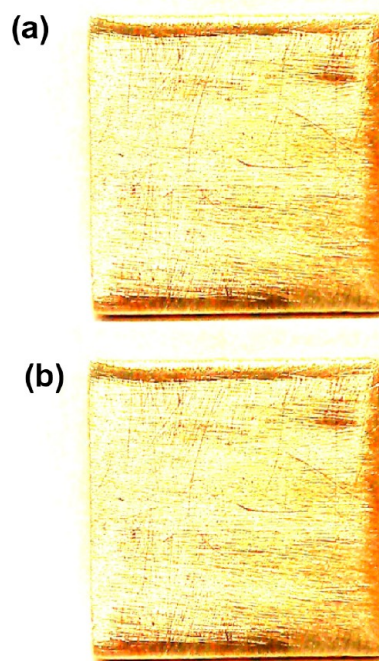

Figure 29. (a) Brass sample after a corrosion test in pure [OMA][DBP]. (b) Brass sample after a corrosion test in pure [OMP][DBP].

than phosphonium ILs, probably due to a different decomposition mechanism at the tribological contact.

The most promising ILs, [OMP][DBP] and [OMA][DBP], show also very favorable corrosion properties as demonstrated in tests with pure IL as well as with water—IL mixtures. In particular, their high compatibility with brass makes them very interesting components for lubricants in industrial applications.

ASSOCIATED CONTENT

Ⓢ Supporting Information

IL characterization, and all analytical details. This material is available free of charge via the Internet at http://pubs.acs.org.

AUTHOR INFORMATION

Corresponding Author

*E-mail: wasserscheid@crt.cbi.uni-erlangen.de. Fax: (+49)-9131-8527421. Tel: (+49)-9131-8527420.

Notes

The authors declare no competing financial interest.
M. Uerdingen is a former employee of Merck KGaA.

ACKNOWLEDGMENTS

■ REFERENCES

(1) Wasserscheid, P.; Welton, T. *Ionic Liquids in Synthesis*; Wiley-VCH Verlag GmbH & Co. KGaA, 2002.

(2) Chiappe, C.; Pieraccini, D. Ionic liquids: Solvent properties and organic reactivity. *J. Phys. Org. Chem.* **2005**, *18*, 275−297.

(3) Aparicio, S.; Atilhan, M.; Karadas, F. Thermophysical properties of pure ionic liquids: Review of present situation. *Ind. Eng. Chem. Res.* **2010**, *49*, 9580−9595.

(4) Ye, C.; Liu, W.; Chen, Y.; Yu, L. Room-temperature ionic liquids: A novel versatile lubricant. *Chem. Commun.* **2001**, 2244−2245.

(5) Minami, I. Ionic liquids in tribology. *Molecules* **2009**, *14*, 2286−2305.

(6) Wang, H.; Lu, Q.; Ye, C.; Liu, W.; Cui, Z. Friction and wear behaviors of ionic liquid of alkylimidazolium hexafluorophosphates as lubricants for steel/steel contacts. *Wear* **2004**, *256*, 44−48.

(7) Jiménez, A. E.; Bermúdez, M. D.; Iglesias, P.; Carrión, F. J.; Martínez-Nicolás, G. 1-N-alkyl-3-methylimidazolium ionic liquids as neat lubricants in steel-aluminium contacts. *Wear* **2006**, *260*, 766−782.

(8) Fox, M. F.; Priest, M. Tribological properties of ionic liquids as lubricants and additives. Part 1: Synergistic tribofilm formation between ionic liquids and tricresyl phosphate. *Proc. Inst. Mech. Eng., Part J* **2008**, *222*, 291−303.

(9) Liu, W.; Ye, C.; Gong, Q.; Wang, H.; Wang, P. Tribological performance of roomtemperature ionic liquids as lubricant. *Tribol. lett.* **2002**, *13*, 81−85.

(10) Lu, Q.; Wang, H.; Ye, C.; Liu, W.; Xue, Q. Room temperature ionic liquid 1-ethyl-3-hexylimidazoliumbis (trifluoromethylsulfonyl)-imide as lubricant for steel/steel. *Tribiol. Int.* **2004**, *37*, 547−552.

(11) Wasserscheid, P.; Uerdingen, M. Ionic liquids as Lubricants. In *Handbook of Green Chemistry*, Vol. 6; Wiley-VCH Verlag GmbH & Co. KGaA, 2010, pp 203−218.

(12) Itoh, T.; Watanabe, N.; Inada, K.; Ishioka, A.; Hayase, S.; Kawatsura, M.; Minami, I.; Mori, S. Design of alkylsulfate ionic liquids for lubricants. *Chem. Lett.* **2009**, *38*, 64−65.

(13) Shah, F. U.; Glavatskih, S.; Antzutkin, O. N. Boron in tribology: From borates to ionic liquids. *Tribol. Lett.* **2013**, *51*, 281−301.

(14) Kuhlmann, E.; Himmler, S.; Giebelhaus, H.; Wasserscheid, P. Imidazolium dialkylphosphates − A class of versatile, halogen-free and hydrolytically stable ionic liquids. *Green Chem.* **2007**, *9*, 233.

(15) Ritchie, C.; Seddon, K. R. *Lubricating Oil Compositions and Uses.* World Patent WO2008075016 A1, 2008.

(16) Zhang, L.; Feng, D.; Xu, B. Tribological characteristics of alkylimidazolium diethyl phosphates ionic liquids as lubricants for steel-steel. *Tribol. Lett.* **2009**, *34*, 95−101.

(17) Yu, B.; Bansal, D.; Qu, J.; Sun, X.; Luo, H.; Dai, S.; Blau, P.; Bunting, B.; Mordukhovich, G.; Smolenski, D. Oil-miscible and non-corrosive phosphonium-based ionic liquids as candidate lubricant additives. *Wear* **2012**, *289*, 58−64.

(18) Yao, M.; Liang, Y.; Xia, Y.; Zhou, F. Bisimidazolium ionic liquids as the high-performance antiwear additives in poly(ethylene glycol) for steel-steel contacts. *ACS Appl. Mater. Interfaces* **2009**, *1*, 467−471.

(19) Zhou, F.; Liang, Y.; Liu, W. Ionic liquid lubricants: Designed chemistry for engineering applications. *Chem. Soc. Rev.* **2009**, *38*, 2590−2599.

(20) Somers, A.; Howlett, P.; MacFarlane, D.; Forsyth, M. A review of ionic liquid lubricants. *Lubricants* **2013**, *1*, 3−21.

(21) Fraser, K. J.; MacFarlane, D. R. Phosphonium-based ionic liquids: An overview. *Aust. J. Chem.* **2009**, *62*, 309−321.

(22) Totten, G. E.; Westbrook, S. R.; Shah, R. J. *Fuels and Lubricants Handbook: Technology, Properties, Performance, and Testing*; American Society for Testing & Materials, 2003.

(23) Seddon, K. R.; Stark, A.; Torres, M.-J. Influence of chloride, water, and organic solvents on the physical properties of ionic liquids. *Pure Appl. Chem.* **2000**, *72*, 2275−2287.

(24) Qu, J.; Bansal, D. G.; Yu, B.; Howe, J. Y.; Luo, H.; Dai, S.; Li, H.; Blau, P. J.; Bunting, B. G.; Mordukhovich, G.; Smolenski, D. J. Antiwear performance and mechanism of an oil-miscible ionic liquid as a lubricant additive. *ACS Appl. Mater. Interfaces* **2012**, *4*, 997−1002.

(25) Qu, J.; Luo, H.; Chi, M.; Ma, C.; Blau, P. J.; Dai, S.; Viola, M. B. Comparison of an oil-miscible ionic liquid and ZDDP as a lubricant anti-wear additive. *Tribol. Int.* **2014**, *71*, 88−97.

(26) Qu, J.; Truhan, J.; Dai, S.; Luo, H.; Blau, P. J. Ionic liquids with ammonium cations as lubricants or additives. *Tribol. Lett.* **2006**, *22*, 207−214.

(27) Elsentriecy, H. H.; Luo, H.; Meyer, M.; Grado, L. L.; Qu, J. Effects of pretreatment and process temperature of a conversion coating produced by an aprotic ammonium-phosphate ionic liquid on magnesium corrosion protection. *Electrochim. Acta* **2014**, *123*, 58−65.

(28) Sun, J. Z.; Howlett, P. C.; MacFarlane, D. R.; Lin, J.; Forsyth, M. Synthesis and physical property characterisation of phosphonium ionic liquids based onP(O)2(OR)2 and P(O)2(R)2 anions with potential application for corrosion mitigation of magnesium alloys. *Electrochim. Acta* **2008**, *54*, 254−260.

(29) Cassol, C. C.; Ebeling, G.; Ferrera, B.; Dupont, J. A simple and practical method for the preparation and purity determination of halide-free imidazolium ionic liquids. *Adv. Synth. Catal.* **2006**, *348*, 243−248.

(30) Maase, M.; Massonne, K.; Szarvas, L. Method for producing ionic liquids World Patent WO 2005070896 A1, 2005.

(31) Kotschan, M.; Kalb, R. Verfahren zur Herstellung ionischer Flüssigkeiten, ionischer Feststoffe oder Gemische derselben. European Patent EP 2295398 A1, 2011.

(32) Selva, M.; Fabris, M.; Lucchini, V.; Perosa, A.; Noe, M. The reaction of primary aromatic amines with alkylene carbonates for the selective synthesis of bis-N-(2-hydroxy)alkylanilines: The catalytic effect of phosphonium-based ionic liquids. *Org. Biomol. Chem.* **2010**, *8*, 5187−5198.

(33) Behrendt, W.; Gattow, G. Über Chalkogenolate. LXII. Untersuchungen über Halbester der Kohlensäure 2. Darstellung und eigenschaften der monomethylkohlensäure. *Z. Anorg. Allg. Chem.* **1973**, *398*, 198−206.

(34) Himmler, S.; König, A.; Wasserscheid, P. Synthesis of [EMIM]OH via bipolar membrane electrodialysis - Precursor production for the combinatorial synthesis of [EMIM]-based ionic liquids. *Green Chem.* **2007**, *9*, 935.

(35) Stribeck, R. Die Wesentlichen eigenschaften der Gleit- und Rollenlager. *Z. Verein. Deut. Ing.* **1902**, *46*, 1341−1348.

(36) Tsunashima, K.; Sugiya, M. Physical and electrochemical properties of low-viscosity phosphonium ionic liquids as potential electrolytes. *Electrochem. Commun.* **2007**, *9*, 2353−2358.

(37) Borruto, A.; Crivellone, G.; Marani, F. Influence of wettability on friction and wear tests. *Wear* **1998**, *222*, 57−65.

(38) Kosmulski, M.; Gustafsson, J.; Rosenholm, J. B. Thermal stability of low temperature ionic liquids revisited. *Thermochim. Acta* **2004**, *412*, 47−53.

(39) Bradaric, C. J.; Downard, A.; Kennedy, C.; Robertson, A. J.; Zhou, Y. Industrial preparation of phosphonium ionic liquids. *Green Chem.* **2003**, *5*, 143−152.

(40) Uerdingen, M.; Treber, C.; Balser, M.; Schmitt, G.; Werner, C. Corrosion behaviour of ionic liquids. *Green Chem.* **2005**, *7*, 321.